

# LINEAR STABILITY ANALYSIS AND CFD SIMULATION OF DOUBLE-LAYER RAYLEIGH- BÉNARD CONVECTION

É. Fontana<sup>1,2\*</sup>, E. Mancusi<sup>1,3</sup>, A. A. Ulson De Souza<sup>1</sup> and S. M. A. Guelli U. Souza<sup>1</sup>

<sup>1</sup>Universidade Federal de Santa Catarina, Departamento de Engenharia  
Química e de Alimentos, 88040-970, Florianópolis - SC, Brazil.

Phone/Fax: (55) (48) 3721 3375

\*E-mail: eliton.fontana@ufsc.br

E-mail: antonio.augusto.souza@ufsc.br; selene.souza@ufsc.br

<sup>2</sup>Universidade Federal de Santa Catarina, Campus Blumenau, 89065-300, Blumenau - SC, Brazil.

<sup>3</sup>Università del Sannio, Facoltà di Ingegneria, 82100 Benevento, Italy.

E-mail: mancusi.erasmo@gmail.com

(Submitted: January 26, 2015 ; Revised: June 1, 2015 ; Accepted: September 12, 2015)

**Abstract** - Natural convection in superimposed layers of fluids heated from below is commonly observed in many industrial and natural situations, such as crystal growth, co-extrusion processes and atmospheric flow. The stability analysis of this system reveals a complex dynamic behavior, including the potential multiplicity of stationary states and occurrence of periodic regimes. In this study, a linear stability analysis (LSA) was performed to determine the onset of natural convection as a function of imposed boundary conditions, geometrical configuration and specific perturbations. To investigate the effects of the non-linear terms neglected in LSA, a direct simulation of the full nonlinear problem was performed using computational fluid dynamics (CFD) techniques. The numerical simulation results show an excellent agreement with the LSA results near the onset of convection and an increase in the deviation as the Rayleigh number increases above the critical value.

**Keywords:** Hydrodynamic Stability; Natural Convection; Multiphase Flow.

## INTRODUCTION

Single layer Rayleigh-Bénard (RB) convection is one of the most widely studied systems in the field of transport phenomena, mainly due to the large number of applications and the relative simplicity of the governing equations. This system represents a natural convection condition occurring in a horizontal layer of fluid where energy is added from below and removed from above, giving rise to cellular structures called Bénard cells (or convective cells) when the buoyancy forces are sufficiently stronger than the viscous forces. Even though it has been investigated for more than a century, the RB problem has been the subject of a large number of studies in recent years,

involving, in particular, modifications of the classical RB system. For example, the problem of natural and mixed convection in enclosures is very important in the study of the cooling of electronic devices and thermal comfort (Fontana *et al.*, 2015; An *et al.*, 2013; Mariani and Coelho, 2007).

The theoretical framework for Rayleigh-Bénard convection was presented by Lord Rayleigh in 1916, based on experimental results obtained by Bénard 16 years earlier. Rayleigh showed that the system stability is governed by a dimensionless parameter, later known as the Rayleigh number ( $Ra$ ), which represents precisely the ratio between buoyancy and viscous forces. Whenever the Rayleigh number is below a certain critical value, the heat transfer will occur

\*To whom correspondence should be addressed

This is an extended version of the work presented at the 20th Brazilian Congress of Chemical Engineering, COBEQ-2014, Florianópolis, Brazil.

basically by conduction. However, when this critical value is exceeded the system becomes unstable and evolves to a different equilibrium state where natural convection is the main heat transfer mechanism. In bifurcation theory terminology, under this condition a bifurcation occurs and the critical point corresponds to a bifurcation point.

Different methods can be applied to investigate the RB system stability, and linear stability analysis (LSA) one of the most commonly used. Although the basics of LSA were first described more than a century ago, this method is still a very useful and powerful tool which is widely used in the study of fluid dynamics systems (e.g., Sahu and Matar, 2010; Fontana *et al.*, 2015a; Sahu and Govindarajan, 2012; Travníkov *et al.*, 2015). Due to a rapid increase in the data processing capacity, LSA studies are reaching a new frontier where the stability of more complex systems can be analyzed in a short amount of time. However, there are drawbacks associated with LSA, especially due to the non-linear terms neglected in this method of analysis. The main objective of this study was to compare the LSA results with CFD simulations carried out using state-of-the-art software packages where the full non-linear form of the governing equations is considered.

Through linear stability analysis it is possible to define the critical Rayleigh values ( $Ra_c$ ) as well as the wavenumber associated with the perturbation that first makes the RB system unstable ( $\alpha_c$ ). As described by Pellew and Southwell (1940), for unbound two-dimensional systems with Newtonian fluids, the critical parameters are governed only by the boundary conditions applied to the velocity vectors at both horizontal boundaries, which can be treated as rigid walls or free surfaces. The values obtained considering the possible combinations, summarized in Table 1, show that the presence of a rigid wall significantly increases the critical parameters, stabilizing the system. In the CFD simulations, the change in the steady-state condition can be observed by a sudden increase in the Nusselt number as the Rayleigh number is increased. When conduction is the only heat transfer mechanism, the Nusselt number is constant, while the presence of convective motion causes an increase in the Nusselt number.

The presence of a second fluid layer significantly increases the system complexity and can affect the stability in many ways, for example, through competition between convective modes in each layer, control of the flow in one layer over the flow in the other, interface deformation and unstable convective modes controlled by interfacial tension gradients. Several

important aspects of the stability of multi-layer fluid systems have been known for decades, for example, those related to the Kelvin-Helmholtz and Rayleigh-Taylor instabilities (Chandrasekhar, 1961). Nevertheless, due to the complex dynamic behavior and the large number of governing parameters, stability analysis of the flow involving superimposed layers of fluids has been studied by several authors in recent years (Mishra *et al.*, 2012; Kushnir *et al.*, 2014; Sahu and Govindarajan, 2011; Redapangu *et al.*, 2012) and is still an ongoing topic in the field of fluid dynamics.

**Table 1: Critical parameters for single layer Rayleigh-Bénard convection (Pellew and Southwell, 1940).**

Boundary condition	$Ra_c$	$\alpha_c$
Rigid – rigid	1707.8	3.117
Rigid – free	1100.7	2.682
Free – free	657.5	2.221

Besides the theoretical importance in the field of stability analysis, the study of the stability of natural convection in multi-layer systems plays an important role in several practical applications, as noted by Anderek *et al.* (1998). Systems where stratification occurs due to differences in density or thermal properties are fairly common in the analysis of geophysical systems, atmospheric flow, astrophysics and industrial processes. The study of these systems was originally motivated by the hypothesis that the Earth's mantle is stratified as a result of a seismic discontinuity observed at a depth of approximately 660 km (Ogawa, 2008). In recent decades the study of double-layer natural convection was extended to several technological applications of significant interest in the chemical engineering field, such as liquid encapsulated techniques for crystal growth (Li *et al.*, 2009), the processing of glass and dispersion materials (Prakash, 1997), micro-channel chemical reactors (Fudym *et al.*, 2007) and the processing of electronic materials under micro-gravity conditions (Gupta *et al.*, 2007).

In the stability analysis of double-layer RB convection several mechanisms that can make the system unstable need to be considered, and in most cases these mechanisms are associated with different time and length scales, particularly when the difference in the depth of each layer or in the physical properties of the fluids in each layer is significant. Therefore, a global analysis considering all of the possible mechanisms cannot be easily carried out using a single method. As previously mentioned, LSA is among the most commonly used methods of hydrodynamic

stability analysis due to its relative simplicity and flexibility. However, this method has intrinsic limitations derived from the fact that high-order terms are neglected in the linearization process. In this study, direct simulation of the full non-linear set of governing equations using modern computational fluid dynamics (CFD)-based techniques was performed and the results compared with those obtained through linear stability analysis (LSA) in order to evaluate the comparative performance of each method.

## MATHEMATICAL MODEL

A scheme of the geometrical configuration considered is shown in Figure 1. The system consists of two layers of immiscible fluids confined between horizontal rigid walls. The system is assumed to be unbound in the  $z$  and  $x$  directions; however, perturbations in these directions are also included in the model. The thickness of the lower layer,  $d_1$ , is used as the length scale with the bottom wall placed at the dimensionless position  $y = -1$  and the upper wall placed at  $y = d_2 / d_1 = d_0$ , where  $d_2$  represents the height of the upper layer. The temperatures of these two walls are considered to be constant and the analysis was limited to the case  $T_H > T_C$  where  $T_H$  is the temperature of the bottom wall and  $T_C$  the temperature of the top wall. The non-deformed interface is positioned at  $y = 0$  and the interface deformation is evaluated using the function  $\eta = \eta(x, z, t)$ .

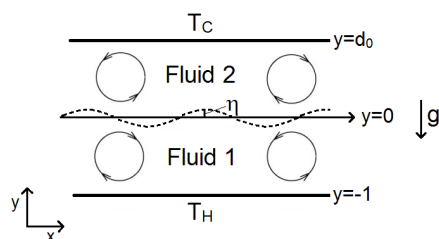


**Figure 1:** Physical domain.

Each layer has its own set of governing equations, these equations being linked by the boundary conditions at the interface. It is assumed that the flow in both layers is incompressible, the fluids have Newtonian behavior and the Boussinesq approximation is valid for the entire range of conditions evaluated. Under these conditions the governing equations are the standard Navier-Stokes and energy and mass conservation equations. No-slip and no-penetration boundary conditions are applied to the velocity vector at the solid walls ( $y = -1$  and  $y = d_0$ ), while fixed

temperatures are defined at the same locations. At the interface ( $y = \eta$ ), conditions of normal and tangential velocity continuity, as well as the shear and normal stress balance, are used to determine the velocity field, while for the energy conservation equation conditions of temperature and heat flux continuity are assumed.

In order to characterize the stability properties of a given base state through linear stability analysis, the variables in the set of governing equations are expressed as the sum of the base state and an infinitesimal perturbation, and thus the dynamic behavior of these perturbations can be used to define the state stability: if the perturbations decrease over time and eventually disappear the system will be stable, otherwise it will be unstable. In LSA only infinitesimal perturbations are considered and thus all of the high-order terms can be neglected. Moreover, non-dimensional variables will be introduced by using  $d_1$  as the length scale,  $\kappa_1 / d_1$  as the scale for the perturbation velocity,  $\rho_1 \nu_1 \kappa_1 / d_1^2$  for the pressure and  $\psi_1 d_1$  as the scale for the temperature, where  $\kappa_1$ ,  $\rho_1$  and  $\nu_1$  are, respectively, the thermal diffusivity, density and kinematic viscosity of the lower layer and  $\psi_1$  is the static temperature gradient between the non-deformed interface and the bottom wall.

The base state represents a solution for the set of governing equations and the related boundary conditions. In this case, the base state is associated with the horizontal velocity ( $U_{B,1}, U_{B,2}$ ) and temperature ( $T_{B,1}, T_{B,2}$ ) in the lower (1) and upper (2) layers. To determine the onset of natural convection in a double-layer RB convection system, the base state corresponds to the stationary fluid ( $U_{B,1} = U_{B,2} = 0$ ) with a linear temperature profile associated with heat transfer only by conduction, given by:

$$T_{B,1} = T_H - \psi_1(y + 1) \quad (1)$$

$$T_{B,2} = T_C - \psi_2(y - d_0) \quad (2)$$

where  $\psi_2$  is the static temperature gradient between the top wall and the non-deformed interface.

For an equilibrium point to be considered stable it needs to be stable with respect to any possible infinitesimal perturbation, otherwise it is unstable. As described by Chandrasekhar (1961), one way to analyze the influence of any possible perturbation is to express the perturbed variables in terms of normal modes. For example, a generic variable  $s$  can be expressed as:

$$s(x, y, z, t) = \bar{s}(y)e^{i(\alpha x + \beta z - \omega t)} \quad (3)$$

where  $\bar{s}(y)$  is the eigenfunction associated with the original variable,  $\alpha$  and  $\beta$  are wavenumbers in the  $x$  and  $z$  directions, respectively, and  $\omega = \omega_r + i\omega_i$  is the wave velocity, where  $\omega_r$  is the phase velocity and  $\omega_i$  the temporal growth rate of the perturbation. A condition where  $\omega_i < 0$  represents a damped perturbation and a stable system, while in cases where  $\omega_i > 0$  the perturbation will grow and the base state will be unstable. The condition  $\omega_i = 0$  is called *neutral stability* and represents a bifurcation point where the change in the steady-state solution occurs. The main objective of LSA is to obtain the values for the parameters where this bifurcation point occurs. In this study, we limit our analysis to temporal instabilities. Thus, the wavenumbers  $\alpha$  and  $\beta$  are real values, which are used as parameters to find the critical Rayleigh number.

After some manipulation, the pressure can be eliminated and the equations governing the system stability in the lower layer can be expressed as (see Fontana (2014) and Fontana *et al.* (2015a) for details):

$$-\frac{i\omega}{\text{Pr}} \left( \frac{d^2 \phi_1}{dy^2} - k^2 \phi_1 \right) = \frac{d^4 \phi_1}{dy^4} - 2k^2 \frac{d^2 \phi_1}{dy^2} + k^4 \phi_1 - k^2 Ra \phi_1 \quad (4)$$

$$-i\omega \theta_1 - \phi_1 = \frac{d^2 \theta_1}{dy^2} - k^2 \theta_1 \quad (5)$$

where  $\phi_1$  and  $\theta_1$  represent the perturbation of the vertical velocity and temperature, respectively,  $k^2$  is defined as  $k^2 = \alpha^2 + \beta^2$  and the Prandtl and Rayleigh numbers are given by:

$$\text{Pr} = \frac{\nu_1}{\kappa_1} \quad Ra = \frac{\beta_1 g \nu_1 d_1^4}{\nu_1 \kappa_1} \quad (6)$$

where  $\beta_1$  is the coefficient of thermal expansivity of the lower layer and  $g$  is the gravitational acceleration. The equations for the upper layer (denoted by the subscript 2) can be expressed as:

$$\begin{aligned} & -\frac{i\omega}{\text{Pr}} \left( \frac{d^2 \phi_2}{dy^2} - k^2 \phi_2 \right) \\ & = \nu_0 \left( \frac{d^4 \phi_2}{dy^4} - 2k^2 \frac{d^2 \phi_2}{dy^2} + k^4 \phi_2 \right) - \beta_0 k^2 Ra \theta_2 \end{aligned} \quad (7)$$

$$-i\omega \theta_2 - \psi_0 \phi_2 = \kappa_0 \left( \frac{d^2 \theta_2}{dy^2} - k^2 \theta_2 \right) \quad (8)$$

where the subscript 0 denotes the relation between the parameter evaluated at the upper and at the lower layer.

As demonstrated by Hesla *et al.* (1986), when the fluids are considered incompressible, homogeneous, immiscible and with constant interfacial tension, Squire's theorem is valid and only two-dimensional perturbations need to be considered to determine the lowest Rayleigh value where the system becomes unstable. Therefore, the condition  $\beta = 0$  will be used to determine the system stability, which implies that  $k^2 = \alpha^2$ .

The no-penetration condition applied at the solid walls ( $y = -1$  and  $y = d_0$ ) can be expressed as:

$$\phi_1 = \phi_2 = 0 \quad (9)$$

while the no-slip conditions gives:

$$\frac{d\phi_1}{dy} = \frac{d\phi_2}{dy} = 0 \quad (10)$$

At the non-deformed interface ( $y = 0$ ), the continuity of normal and tangential velocities, respectively, is given by:

$$\phi_1 = \phi_2 \quad (11)$$

$$\frac{d\phi_1}{dy} = \frac{d\phi_2}{dy} = 0 \quad (12)$$

The continuity of shear stress at the interface (neglecting the thermocapillary effect) results in:

$$\left( k^2 \phi_1 + \frac{d^2 \phi_1}{dy^2} \right) - m \left( k^2 \phi_2 + \frac{d^2 \phi_2}{dy^2} \right) = \eta_0 k^2 \quad (13)$$

where  $m$  is the relation between the dynamic viscosity in the upper and lower layers and  $\eta_0$  is the dimensionless interface deformation expressed in terms of normal modes. Using the kinematic condition,  $\eta_0$  can be expressed as:

$$\eta_0 = \frac{\phi_1(0)}{i\omega} \quad (14)$$

The last boundary condition for Equations (4) and

(7) is the balance of normal stress at the interface, given by:

$$\left( \frac{d^3 \phi_1}{dy^3} - 3k^2 \frac{d\phi_1}{dy} - \frac{\omega}{Pr} \frac{d\phi_1}{dy} \right) - m \left( \frac{d^3 \phi_2}{dy^3} - 3k^2 \frac{d\phi_2}{dy} - \frac{\omega}{\nu_0 Pr} \frac{d\phi_2}{dy} \right) = \eta_0 k^2 (Ra_\rho + k^2 S) \quad (15)$$

where the interfacial tension-based Schmidt ( $S$ ) number and a Rayleigh number based on the density difference between the upper and lower layers ( $Ra_\rho$ ) are defined as:

$$Ma = -\frac{d\gamma}{dT} \frac{\psi_1 d_1^2}{\nu_1 \rho_1 \kappa_1} \quad S = \frac{\gamma d_1}{\nu_1 \rho_1 \kappa_1} \quad (16)$$

$$Ra_\rho = \frac{g d_1^3}{\nu_1 \kappa_1} \left( 1 - \frac{\rho_2}{\rho_1} \right)$$

where  $\gamma$  is the interfacial tension and  $T$  is the temperature.

The conditions of fixed temperature at the solid walls ( $y = -1$  and  $y = d_0$ ) are expressed as:

$$\theta_1 = \theta_2 = 0 \quad (17)$$

while the conditions of continuity of temperature and heat flux at the interface give, respectively:

$$\theta_1 - \theta_2 = \eta_0 (1 - \psi_0) \quad (18)$$

$$\frac{d\theta_1}{dy} = k_0 \frac{d\theta_2}{dy} \quad (19)$$

To solve the generalized eigenvalue problem obtained, a pseudo-spectral method using Chebyshev polynomials was applied (see Canuto *et al.* (2006) for further details). For example, the perturbation in the temperature of the bottom layer,  $\theta_1$ , is expressed as:

$$\theta = \sum_{k=0}^{N-1} \bar{\theta}_1^k T_k(y) \quad (20)$$

where  $T_k$  is the Chebyshev polynomial of order  $k$  and  $\bar{\theta}_1^k$  is the coefficient associated with  $T_k$ . To validate

the resolution methodology, stability curves obtained with the proposed method were compared with results reported by Cardin *et al.* (1991), as seen in Figure 2. An excellent agreement between the results can be observed, even considering the existence of a periodic state. The two branches of solution observed in this figure correspond to the two most unstable modes and the merging of these branches through a Hopf bifurcation gives rise to the periodic state.

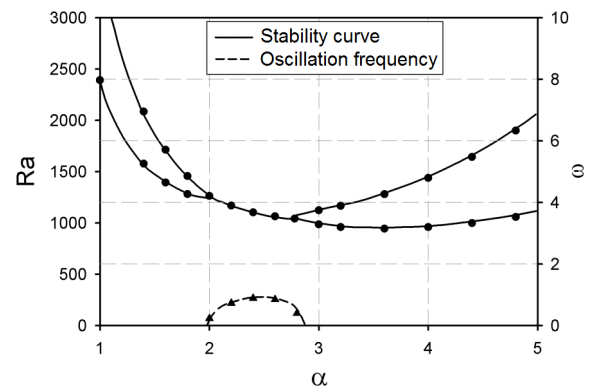


**Figure 2:** Comparison between the stability curves presented by Cardin *et al.* (1991) (lines) and those obtained with the proposed methodology (points). These results correspond to the case  $d_0 = 0.76$ ,  $k_0 = 0.54$ ,  $\rho_0 = 0.77$ ,  $\kappa_0 = 1.27$ ,  $\nu_0 = 0.67$ ,  $\alpha_0 = 1.92$ ,  $Pr = 8400$ ,  $S = 0$  and  $Ra_\rho^{-1} = 0$ .

Direct simulation analysis based on CFD techniques was performed using the ANSYS Fluent 14.0 software, where the set of governing equations is discretized through a multigrid finite volume approach. The ANSYS-CFD package is widely used to solve natural convection problems with high accuracy (see Fontana *et al.* (2011, 2013a) and Ghalambaz *et al.* (2014), for example). The hypothesis applied, the governing equations and the boundary conditions applied at the solid walls used in the CFD simulation are the same as those previously described for the LSA. To evaluate the interface deformation, the volume of fluid (VOF) method was used. This method computes the interface position based on the velocity and pressure fields and therefore it is not necessary to specify the interface shape or even the boundary conditions at the interface, since these are directly obtained by the method. Further details regarding the VOF method can be found in Fontana *et al.* (2013) and Mancusi *et al.* (2014). A grid convergence test was performed and we found that a mesh with around  $10^5$  elements is sufficient to keep the solution stable and provide the desired convergence criteria of  $10^{-6}$ . A

non-uniform elements distribution was used, with a greater concentration of elements close to the interface and the solid walls, where more intense gradients in the field variables are expected. To define the time-steps used, the Courant number was set to one. This condition resulted in time-steps of the order of seconds, depending on the intensity of the convective motion.

## RESULTS

The physical properties were chosen so that the Rayleigh numbers for the two layers were the same when  $d_0 = 1.0$  ( $\alpha_0 = 1$ ,  $\nu_0 = 1$ ,  $\kappa_0 = 1$ ,  $\rho_0 = 1$  and  $k_0 = 1$ ). Unless otherwise stated, these values were used to obtain all results discussed below. Moreover, the conditions  $Pr = 1$  and  $Ra_\rho = 10^5$  are considered.

This  $Ra_\rho$  value corresponds to a common value found in the laboratory experiments. As noted by Govindarajan and Sahu (2014), one of the most important parameters in double-layer convection is the viscosity difference in each layer. Thus, several authors have investigated the effect of a viscosity difference in double-layer Rayleigh-Bénard convection (see Rasenat *et al.* (1988) and Cardin *et al.* (1991), for example). In this paper, we also assume that  $m = 1$  in order to investigate the effect of the other parameters, in particular the relation between the thickness of each layer.

Figure 3 shows the stability limit curve obtained through LSA, where the critical Rayleigh number is presented as a function of the depth of the upper layer ( $d_0$ ). The points obtained by CFD simulation for several  $d_0$  values are also reported in Figure 3. These points are classified as stable or unstable, depending on the presence or not of convective motion.

As can be seen in Figure 3, the limits defined by

the linear stability analysis are in excellent agreement with the results of the CFD simulations, with only one stable point appearing in the unstable region. However, around the critical value, the onset of convection is not easily defined in the CFD simulations, since a theoretically infinite time would be necessary for a stationary convective state to be developed. It should be noted that the  $Ra_c$  values obtained in the cases  $d_0 = 0.0$  and  $d_0 = 1.0$  correspond exactly to the values for the critical Rayleigh number for single layer RB convection when, respectively, rigid-rigid walls and rigid wall-free surface conditions are considered (see Table 1). This indicates complete consistency between the double and single-layer models.

Besides the onset of convection, the LSA allows the spatial distribution of the velocity and temperature fields to be obtained through eigenfunctions. A comparison between these eigenfunctions and the actual velocity and temperature profiles (deviation from the base state) obtained from the CFD simulations is shown in Figure 4 for  $d_0 = 0.8$  and  $Ra$  close to the critical value.

The profiles obtained from the LSA and the CFD simulation of the full nonlinear problem show excellent agreement, in particular in relation to the velocity profiles. Despite a small deviation in the magnitude in comparison with the CFD results, the LSA eigenfunctions of the temperature deviation show the same tendency. A small change in the Rayleigh number does not affect significantly the profiles in any of the cases. A consistency in the eigenfunctions can also be observed for different  $d_0$  values, as reported in Figure 5. The Rayleigh values adopted for each case correspond to the unstable point closest to the critical point in Figure 3. These results show that, despite all of the simplifications and approximations made in the linearization process, LSA is able to describe very well the system behavior near the critical point.

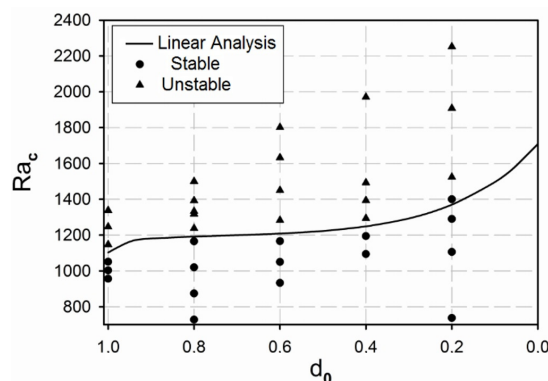


**Figure 3:** Comparison between stability limits obtained through LSA (line) and DNS (points).

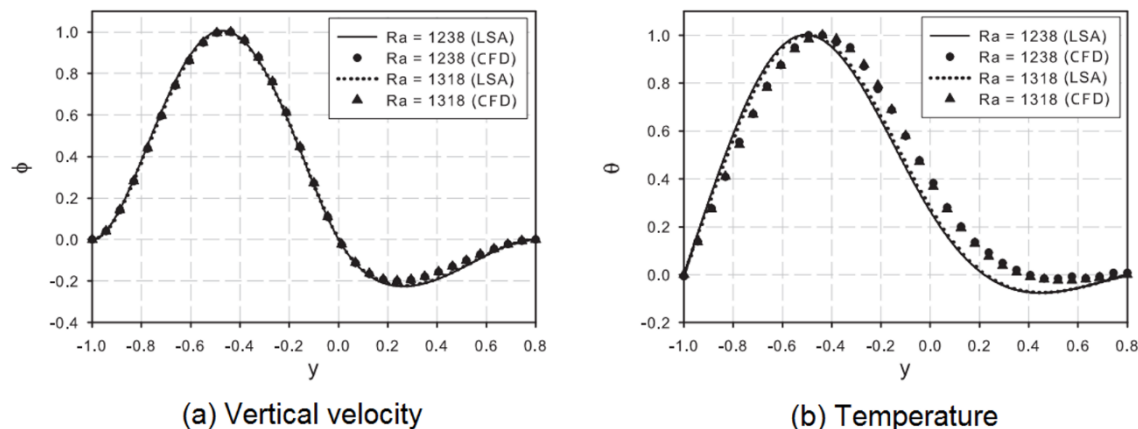


**Figure 4:** Comparison between eigenfunctions obtained through LSA and velocity and temperature profiles obtained with CFD simulations for  $d_0 = 0.8$ .

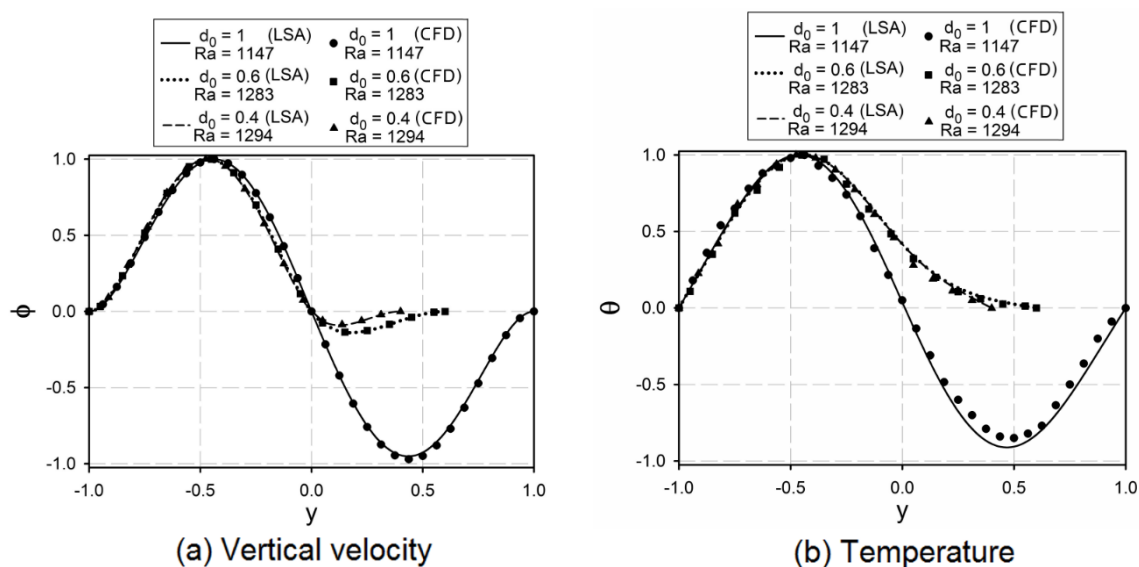


**Figure 5:** Comparison between eigenfunctions obtained through LSA and velocity and temperature profiles obtained with CFD simulations  $d_0 = 1.0, 0.6$  and  $0.4$ .

One of the most restrictive hypothesis of the LSA using normal modes is that the interface deformation is not strong enough for the high-order terms to be neglected. In other words, this condition can be expressed as  $\eta \ll d_1$ . On the other hand, the main advantage of using the VOF method to investigate double-layer convection is that it is possible to track the interface position at each point as a function of the velocity and temperature fields. The interface deformation is controlled by the normal stress balance, in particular by the value of  $Ra_\rho$ . If this value is not high enough to keep the interface stable, surface waves will emerge and eventually the system will

shift to an unstable state. The condition  $Ra_\rho < 0$  will not be considered since it represents, by definition, a Rayleigh-Taylor instability condition.

The vertical velocity and temperature deviation profiles, obtained through CFD simulations, are shown in Figure 6 for  $Ra_\rho = 10^3$  and  $d_0 < 1.0$ , together with the interface position for several values of  $Ra_\rho > Ra_c$ . To facilitate the visualization of the results, allowing the use of a single legend, the values for  $Ra = 1425$  were multiplied by a scale, as indicated in the figure for each case.

For  $Ra_\rho = 10^3$  the critical Rayleigh number is

approximately 1163 and therefore the results shown in Figure 6(a) are very close to the critical value. In this case, the interface deformation can be neglected and the velocity and temperature profiles are similar to those obtained at higher  $Ra_\rho$  values. For  $Ra = 1234$  (Figure 6(b)), a small deformation in the interface position can be observed; however, the condition  $\eta \ll d_1$  still holds true and the velocity and temperature profiles are very similar to  $Ra = 1163$ .

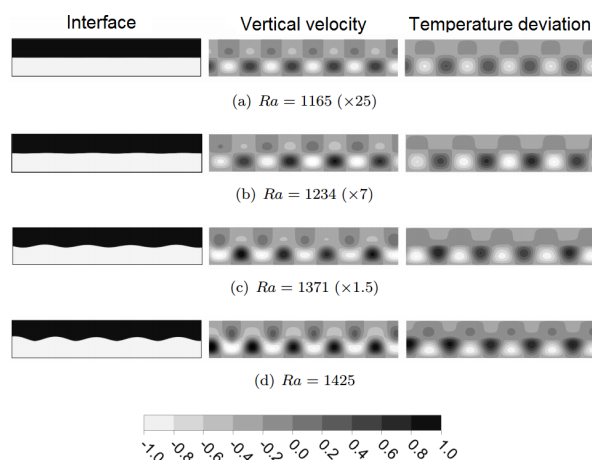


**Figure 6:** Influence of interface deformation on velocity and temperature fields for  $Ra_\rho = 10^3$ .

Even though the interface deformation is negligible when  $Ra$  is close to the critical value, as the Rayleigh number increases it becomes stronger, as seen in Figure 6. For  $Ra = 1371$  (Figure 6(c)) the velocity profiles are significantly different and the convective cells become distorted. The interface acquires a wavy shape, with the maximum points (crest) appearing in the region where the fluid ascends, and the vertical velocity in the lower layer is positive near the interface and the minimum points appear in the descending region. For  $Ra = 1425$  the deformations further increase and the deviation from the linearized model is more significant.

## CONCLUSIONS

In this paper a comparison between linear stability analysis using normal modes and numerical simulation (with CFD techniques) of double-layer Rayleigh-Bénard convection has been presented. LSA techniques allow the determination of the critical value at which the convection starts; however, the linearization process neglects high-order terms and this can lead to deviations from the actual system behavior.

The CFD simulations, on the other hand, solve the full non-linear system of governing equations, but they are much more computationally expensive. The results show that the performance of LSA is excellent near the critical point and thus it can be used to define the critical values. Moreover, at this limit the velocity and temperature profiles obtained with LSA accurately describe the system behavior. However, as the intensity of the convective motion increases, the deviations from the linearized model increase and the velocity and temperature profiles given by the LSA are no longer consistent. In particular, a higher velocity at the interface leads to the development of interfacial waves, causing a strong deformation in the temperature and velocity fields.

## ACKNOWLEDGMENTS

The authors would like to thank the CNPq (*Conselho Nacional de Desenvolvimento Científico e Tecnológico* – Brazil) for financial support through the process 143152/2011-4.

## NOMENCLATURE

$d$	Fluid layer thickness (m)
$g$	Acceleration of gravity ( $\text{m/s}^2$ )
$Pr$	Prandtl number (–)
$Ra$	Rayleigh number (–)
$Ra_\rho$	Density-based Rayleigh number (–)
$S$	Interfacial tension-based Schmidt number (–)
$T$	Temperature (K)
$T_C$	Temperature of the upper wall (cold) (K)
$T_H$	Temperature of the bottom wall (hot) (K)
$T_k$	Chebyshev Polynomial of order $k$ (–)
$U$	Horizontal velocity (m/s)
$x$	Dimensionless horizontal direction (–)
$y$	Dimensionless vertical direction (–)
$z$	Dimensionless transversal direction (–)

## Greek Letters

$\alpha$	Perturbation wavenumber in the x direction (–)
$\beta$	Perturbation wavenumber in the z direction (–)
$\beta_i$	Thermal expansion coefficient of the $i$ -fluid ( $1/\text{K}$ )
$\gamma$	Interfacial tension (N/m)

$\eta$	Interface deformation (m)
$\theta$	Perturbation of the temperature (–)
$\kappa$	Thermal diffusivity (m <sup>2</sup> /s)
$\nu$	Kinematic viscosity (m <sup>2</sup> /s)
$\rho$	Fluid density (kg/m <sup>3</sup> )
$\phi$	Perturbation of the vertical velocity (–)
$\psi$	Static temperature gradient (K)
$\omega$	Wave velocity/eigenvalue (–)

### Subscripts

$B$	Base state
$c$	Critical value
$0$	Ratio between upper and lower layer
$1$	Lower layer
$2$	Upper layer

### REFERENCES

- An, C., Vieira, C. B., Su, J., Integral transform solution of natural convection in a square cavity with volumetric heat generation. *Braz. J. Chem. Eng.*, 30(4), p. 883-896 (2013).
- Anderek, C. D., Colovas, P. W., Degen, M. M., Renardy, Y. Y., Instabilities in two layer Rayleigh-Bénard convection: Overview and outlook. *Int. J. Eng. Sci.*, 36, p. 1451-1470 (1998).
- Canuto, C., Hussaini, M. Y., Quarteroni, A., Zang, T. A., *Spectral Methods: Fundamentals in Single Domains*. [S.I.], Springer (2006).
- Cardin, P., Nataf, H. C., Dewost, P., Thermal coupling in layered convection: evidence for an interface viscosity control for mechanical experiments and marginal stability analysis. *J. Physics II*, 1, p. 599-622 (1991).
- Chandrasekhar, S., *Hydrodynamic and Hydromagnetic Stability*. [S.I.], Clarendon Press (1961).
- Fontana, É., Silva, A., Mariani, V. C., Natural convection in a partially open square cavity with internal heat source: An analysis of the opening mass flow. *Int. J. of Heat and Mass Transfer*, 54, p. 1369-1386 (2011).
- Fontana, É., Mancusi, E., Souza, A. A. U., Souza, S. M. A. G. U., Flow regimes for liquid water transport in a tapered flow channel of proton exchange membrane fuel cells (PEMFCs). *J. Power Sources*, 234, p. 260-271 (2013).
- Fontana, É., Capeletto, C. A., Silva, A., Mariani, V. C., Three-dimensional analysis of natural convection in a partially-open cavity with internal heat source. *Int. J. of Heat and Mass Transfer*, 61, p. 525-542 (2013a).
- Fontana, É., *Análise de estabilidade da convecção de Rayleigh-Bénard-Poiseuille estratificada*. PhD Thesis, Universidade Federal de Santa Catarina (2014). (In Portuguese).
- Fontana, É., Capeletto, C. A., Silva, A., Mariani, V. C., Numerical analysis of mixed convection in partially open cavities heated from below. *Int. J. of Heat and Mass Transfer*, 81, p. 829-845 (2015).
- Fontana, É., Mancusi, E., Souza, A. A. U., Souza, S. M. A. G. U., Stability analysis of stratified Rayleigh-Bénard-Poiseuille convection: Influence of the shear flow. *Chem. Eng. Sci.*, 126, p. 67-79 (2015a).
- Fudym, O., Pradere, C., Batsale, J. C., An analytical two-temperature model for convection-diffusion in multilayered systems: Application to the thermal characterization of microchannel reactors. *Chem. Eng. Sci.*, 62, p. 4054-4064 (2007).
- Ghalambaz, M., Noghrehabadi, A., Ghanbarzadeh, A., Natural convection of nanofluids over a convectively heated vertical plate embedded in a porous medium. *Braz. J. Chem. Eng.*, 31(2), p. 413-427 (2014).
- Govindarajan, R., Sahu, K. C., Instabilities in viscosity-stratified flow. *Annu. Rev. Fluid Mech.*, 46, p. 331-353 (2014).
- Gupta, N. R., Hariri, H. H., Borhan, A., Thermocapillary convection in double-layer fluid structures within a two-dimensional open cavity. *J. of Colloid and Interface Science*, 315, p. 237-347 (2007).
- Hesla, T. I., Pranckh, F. R., Preziosi, L., Squire's theorem for two stratified fluids. *Phys. of Fluids*, 29, p. 2808-2811 (1986).
- Kushnir, R., Segal, V., Ullmann, A., Brauner, B., Inclined two-layered stratified channel flows: Long wave stability analysis of multiple solution regions. *Int. J. Multiphase Flow*, 62, p. 17-29 (2014).
- Li, Y. R., Wang, S. C., Wu, S. Y., Peng, L., Asymptotic solution of thermocapillary convection in thin annular two-layer system with upper free surface. *Int. J. Heat and Mass Transfer*, 52, p. 4769-4777 (2009).
- Mancusi, E., Fontana, E., Ulson de Souza, A. A., Guelli U. Souza, S. M. A., Numerical study of two-phase flow patterns in the gas channel of PEM fuel cells with tapered flow field design. *Int. J. Hydrogen Energy*, 39, p. 2261-2273 (2014).
- Mariani, V. C., Coelho, L. S., Natural convection heat transfer in partially open enclosures containing an internal local heat source. *Braz. J. Chem. Eng.*, 24(3), p. 375-388 (2007).
- Mishra, M., De Wit, A., Sahu, K. C., Double diffusive effects on pressure-driven miscible displacement flows in a channel. *J. Fluid Mech.*, 12, p. 579-597 (2012).

- Ogawa, M., Mantle convection: A review. *Fluid Dynamics Research*, 40, p. 379-398 (2008).
- Pellew, A., Southwell, R. V., On maintained convective motion in a fluid heated from below. *Proc. of the Royal Society*, 176(966), p. 312-342 (1940).
- Prakash, A., Yasuda, K., Otsubo, F., Kuwahara, K., Doi, T., Flow coupling mechanisms in two-layer Rayleigh-Bénard convection. *Experiments in Fluids*, 23, p. 252-261 (1997).
- Rasenat, S., Busse, F. H., Rehberg, I., A theoretical and experimental study of double-layer convection. *J. Fluid Mechanics*, 199, p. 519-540 (1989).
- Redapangu, P. R., Vanka, S. P., Sahu, K. C., Multi-phase lattice Boltzmann simulations of buoyancy-induced flow of two immiscible fluids with different viscosities. *Eur. J. Mech. B/Fluids*, 34, p. 105-114 (2012).
- Sahu, K. C., Govindarajan, R., Linear stability of double-diffusive two-fluid channel flow. *J. Fluid Mech.*, 687, p. 529-539 (2011).
- Sahu, K. C., Govindarajan, R., Spatio-temporal linear stability of double-diffusive two-fluid channel flow. *Phys. Fluids*, 24, 054103 (2012).
- Sahu, K. C., Matar, O. K., Three-dimensional linear instability in pressure-driven two-layer channel flow of a Newtonian and a Herschel-Bulkley fluid. *Physics of Fluids*, 22, 112103 (2010).
- Travnikov, V., Eckert, K., Odenbach, S., Linear stability analysis of the convective flow in a spherical gap with  $\eta = 0.714$ . *Int. J. Heat and Mass Transfer*, 80, p. 266-273 (2015).